UDC 621.9.025.7:621.762.5:661.657.5

T. Kolabylina[1, 2, *], V. Bushlya[2], I. Petrusha[1], D. Johansson[2], J.-E. Ståhl[2], V. Turkevich[1],
[1]Bakul Institute for Superhard Materials,
National Academy of Sciences of Ukraine, Kiev, Ukraine
[2]Division of Production and Materials Engineering, Lund University, Lund, Sweden
**tetiana.kolabylina@chemie.tu-freiberg.de*

Superhard pcBN tool materials with Ti_3SiC_2 MAX-phase binder: structure, properties, application

Superhard cutting tool materials were sintered in cBN–(Ti_3SiC_2–TiC) system via high pressure–high temperature method. Sintering was performed under the pressure 8 GPa in the 1400–2400 °C temperature range. The initial mixtures of three compositions were chosen with 90, 80 and 60 vol % cBN. The mixtures were prepared by mixing cBN (1–3 μm) and Ti_3SiC_2–TiC (< 2 μm). It was found, that upon sintering, the compositions of the obtained samples differed from the initial mixtures in all cases as a result of chemical reactions. Microstructure observations, phase composition estimation, and mechanical properties of the obtained tool materials were carried out. The results indicate that both the varying cBN content and the applied sintering conditions have a direct effect on the structure, properties, and kinetics of reactions.

***Keywords**: pcBN, Ti_3SiC_2 MAX-phase, HPHT.*

INTRODUCTION

The pcBN tool materials have found their applications in machining operations when cutting difficult-to-machine materials and hardened steels [1–3]. ISO 1832:2012 [4] differentiates pcBN materials into grades with low-cBN and high-cBN contents with respective application areas of finish machining and roughing or interrupted cuts. Low-cBN grades often contain TiC, Ti(C,N) or TiN binders [5]. Alternative binding phases, which can handle high temperatures and high level of chemical and abrasive wear, are continuously sought for.

First discovered at 60-th layered ternary carbides (so-called MAX-phases[1]) came back under the spot last decades [6]. Being built of carbide blocks they are still not the same with normal carbides and fall under an intermediate class between metals and ceramics. What makes them behave differently from normal carbides is their structure, which determinates their ability to withstand elevated temperatures, tolerate high stresses, and possess high compactibility of their powder products. Preliminary studies by the authors have shown that compaction

[1] Layered, hexagonal carbides and nitrides with general formula: $Mn+1AX_n$, (MAX phases) where n = 1 to 3, M is an early transition metal, A is an A-group (mostly IIIA and IVA, or groups 13 and 14) element and X is either carbon and/or nitrogen possessing with whole set of needed properties.

rate for commercially available Ti_3SiC_2 and Ti_2AlC MAX-phases is the highest, slightly below their decomposition temperature.

In attempts to introduce these positive MAX-phase properties into tool materials many research studies have involved sintering of superhard tool materials based on diamond or cubic boron nitride with commercially available MAX-phases [7–13].

Multiple sintering techniques were used for production of cutting tool materials. Starting from pressureless sintering [8], hot pressing at pressure 20–35 MPa [13], and up to high pressure–high temperature (HPHT) techniques synthesis [9–11]. In these cases Ti_3SiC_2 MAX-phase was in-situ sintered from starting Ti, Si, SiC, TiC powders together with superhard diamond or cBN filler. Effect of the cBN filler amount on sintering conditions was investigated. For a diamond filler, it was found that the increased diamond content significantly promotes a Ti_3SiC_2 formation [13]. In many cases a partial reverse transformation of diamond and cBN were observed because superhard phases become unstable under conditions required for the efficient MAX-phase sintering [8, 12, 14].

Alternatively, sintering can involve preliminary obtained MAX-phase used as a binder in order to solve the mentioned reverse transformation difficulties. In such a case both MAX-phase and superhard phase need to be preserved while sintering the cutting tool material. Decomposition of MAX-phase needs to be prevented. High pressure sintering was found to provide a solution due to reduced requirements to sintering temperatures, which decreases by approx. one hundred degrees [14] in comparison to other techniques. Additionally, sintering time is significantly shortened.

The application of high pressure may activate decompositions of certain MAX-phases [15]. The use of such MAX-phases as precursors for pcBN tool materials results in multiphase composite material due to chemical reactions. For example in the case of Ti_3SiC_2, depending on sintering conditions TiB_2, TiC, TiN, SiB_3, and SiC phases are expected [9, 10, 16]. This phase composition is somewhat similar to cBN–TiC and cBN–TiN commercial materials. At the same time two main differences can be expected. First, the observed decomposition of Ti_3SiC_2 is expected to result in fine-grained microstructure. Second, this microstructure possesses a multi-phase composition (5–6 phases), where all phases have high hardness.

The aim of this study is to estimate the influence of the sintering conditions and binder content on the structure and properties of the cBN–Ti_3SiC_2–TiC composite. The microstructure, phase composition, and phase stoichiometry as well as the microhardness, fracture toughness, density, and tool material performance are established.

EXPERIMENTAL PROCEDURE

Mixture preparation

Sintering of cutting tool materials both in high-cBN and low-cBN systems was intended.

The compositions of the initial mixtures are listed in Table 1. cBN powder with grain sizes of 1–3 μm was admixed with Ti_3SiC_2 and TiC powders. Ti_3SiC_2 powder was obtained by milling commercial Maxtal 312 ceramic material down to the fineness of 0.2–2 μm. Small amount of graphite and approximately 30 vol % of TiC have been identified in the milled products.

Table 1. The compositions of the initial mixtures

Mixture	Initial components	Volume ratio
1	cBN:Ti_3SiC_2:TiC	90:6:4
2	cBN:Ti_3SiC_2:TiC	80:12:8
3	cBN:Ti_3SiC_2:TiC	60:24:16

Premixing was performed by a triple dry co-mixing of cBN and Ti_3SiC_2–TiC powders through sieves with 20 μm cell size. The final mixing involved wet (isopropanol) mixing in a tumbler mixer in the presence of ZrO_2 grinding bodies for 12 h. Each mixture was quality checked via SEM, XRD and EDX techniques.

Sintering of samples

The samples were sintered in a toroid type high-pressure apparatus HPA-30 [17] at the pressure of 8 GPa. A sintering temperature was selected as a variable and ranged within 1400–2400 °C with step of 200 °C. Upon stabilization of the pressure the sample was heated up to a predefined temperature within 5 s. The duration of the heating cycle at a constant temperature was 45 s, then the power in the circuit was decreased within 10 s and the pressure released. The obtained samples were ground to RNGN090300T cutting insert shape.

Samples characterization

Prior to microscopy and indentation studies the samples were polished with diamond suspension (1 and 9 μm) and silica colloidal solution (0.04 μm). FEI NanoLab 600 dual beam microscope was used to analyze the microstructure. A JSM-6700F microscope was used for the energy dispersive X-ray (EDX) analysis (SDD X-Max^n EDX system, Oxford Instruments). XRD analysis of materials was done on a STOE Darmstadt diffractometer with Cu$K\alpha$ source. The hardness of the tool materials was measured with Vickers and Knoop indenters at a load of 4.9 N on an Ernst Leitz Wetzlar microhardness tester. Fracture toughness was estimated via the indentation technique [18] at 300 N load. The density was defined via hydrostatic weighing.

Cutting performance

Cutting performance was estimated through hard turning tests when dry machining cold work tool steel Vanadis 4E (HRC 59). All tests involved constant conditions: cutting speed $v_c = 150$ m/min, feed $f = 0.1$ mm/rev, depth-of-cut $a_p = 0.2$ mm.

RESULTS

Mixing

The mixtures were found to have different mixing quality. For example, in mixture with 90 vol % cBN the majority of the Ti_3SiC_2–TiC binder (10 vol %) was agglomerated. Sizes of the agglomerates were in the range of 5–15 μm, while the original binder grain size was below 2 μm. The agglomeration of Ti_3SiC_2–TiC was not observed in the mixtures with 80 and 60 vol % of cBN. For all mixtures an additional reduction of grain sizes due to grinding and flaking of MAX-phase was present.

All three prepared mixtures appeared to be contaminated by the presence of small (~ 0.2 μm) ZrO_2 inclusions as detected via EDX. The source of such ZrO_2 contamination is due to milling of zirconia grinding bodies themselves. The amount, size and dispersion of zirconia inclusions was approximately the same for all prepared mixtures. The amount of ZrO_2 was not sufficient to be detected with XRD (Fig. 1). While sintering no reactions between ZrO_2 inclusions and surrounding binder neither with cBN materials were observed. Therefore, the presence of ZrO_2 was not considered further on in the study.

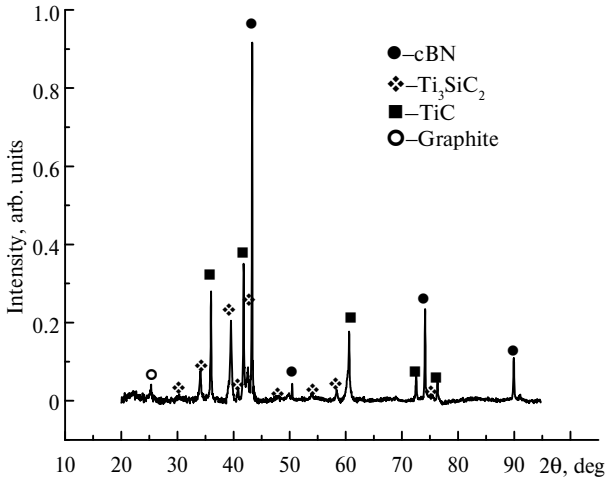

Fig. 1. XRD pattern of the composition of a powder mixture with 60 vol % cBN.

Phase composition of sintered samples

Phase compositions of the sintered samples were determined by the XRD. It was found that the phase compositions of all obtained samples were different from the compositions of the initial mixtures. The main initial binder component Ti_3SiC_2 is not observed in the XRD patterns (Fig. 2), despite the presence of TiC in the initial mixture, which inhibits the Ti_3SiC_2 decomposition [13]. Also several new phases were detected (see Fig. 2).

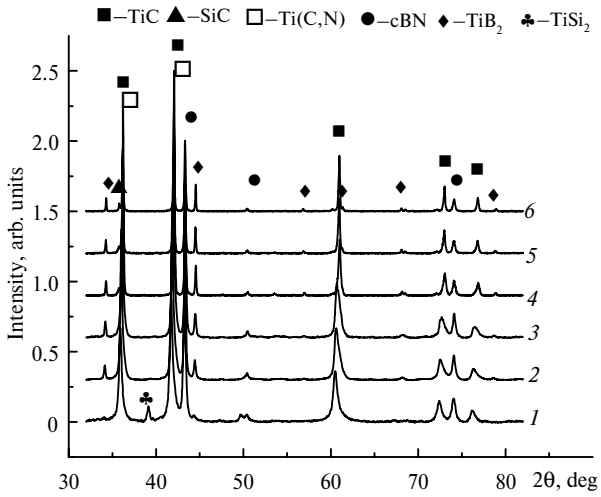

Fig. 2. XRD pattern for 60 vol % cBN samples sintered under different HPHT conditions: 1400 (*1*), 1600 (*2*), 1800 (*3*), 2000 (*4*), 2200 (*5*), 2400 (*6*) °C.

Some of these new phases are determined explicitly, like $TiSi_2$, SiC, and TiB_2. The presence of Ti(C,N) is also confirmed by the XRD, yet the exact stoichiometry described as TiC_xN_y changes with the temperature. More data on the stoichiometry can be obtained through EDX; however, the accuracy for carbon and nitrogen light elements is relatively low for this method.

It is worth noting that the decomposition of $TiSi_2$ still observed at 1400 °C (see Fig. 2) does not result in the formation of Si-containing phases up to 2000 °C. This Si containing phase is SiC. Its low intensity SiC maximum has been detected with XRD only for 60 vol % cBN sample. The EDX data in Fig. 3 confirm the XRD observations by indicating the decomposition of Ti_3SiC_2 at 1400 °C to form $TiSi_2$, TiC, and TiC_xN_y. The majority of $TiSi_2$ grains were found in the central region of Ti_3SiC_2 decomposition and reaction products.

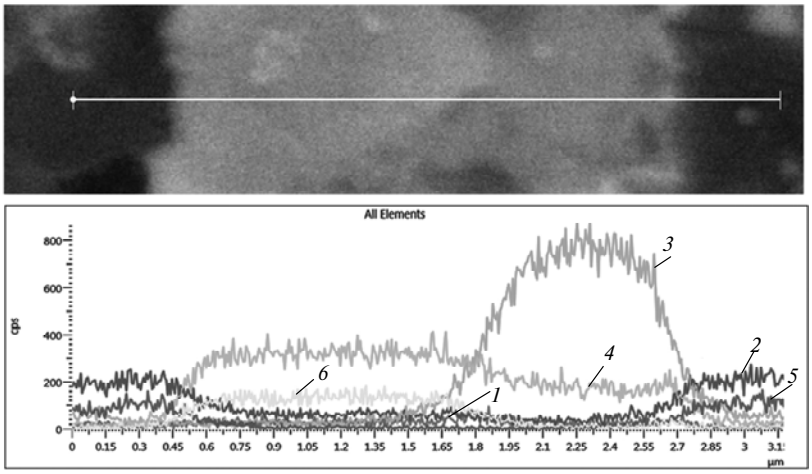

Fig. 3. EDX line-scan data for 80 vol % cBN sample sintered under p = 8 GPa and T = 1400 °C: O$K\alpha_1$ (*1*), N$K\alpha_{1_2}$ (*2*), Si$K\alpha_1$ (*3*), Ti$K\alpha_1$ (*4*), B$K\alpha_{1_2}$ (*5*), C$K\alpha_{1_2}$ (*6*).

As is seen from Fig. 4, the situation changes at the higher sintering temperature of 2400 °C. The EDX line-scan data indicate the formation of SiC also in the central region of the Ti_3SiC_2 decomposition area. It also shows that a nitrogen content in the Ti(C,N) phase found on the sides of SiC has increased the N concentration compared to the case of 1400 °C.

Quantitative point analysis data presented in Fig. 5 indicate that spectrum 31 corresponds to SiC, even though silicon carbide was not observed with the XRD. Data for spectrum 32 confirm the presence of TiB_2 also found with the X-ray diffraction.

Additionally, the EDX data indicate the presence of oxygen, which in the average corresponds to approx. 2 at % for this sample sintered at 2400 °C. Similar analysis for other samples sintered at different temperatures shows that higher oxygen amount of up to 4 at % was present for T = 1400 to 1800 °C. For the entire temperature range above 1800 °C the oxygen content decreases almost twice.

Possible reactions between the initial components of the mixture under given sintering conditions have already been reported [6, 13]:

$$TiC + Ti_3SiC_2 \rightarrow TiC + Ti_xC_y + TiSi_2; \quad (1)$$

$$cBN + TiC + Ti_xC_y + TiSi_2 \rightarrow cBN + TiC + Ti_xC_y + SiC + Ti_zC_v(N) + TiB_2 + Si_{amorf}. \quad (2)$$

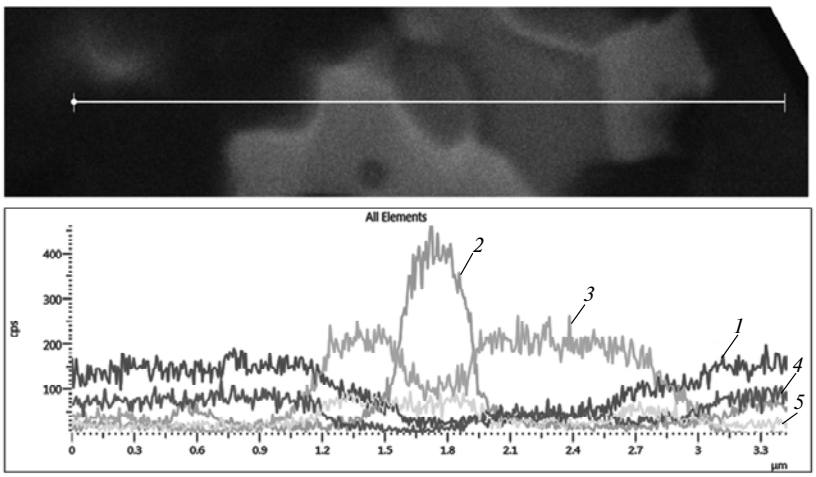

Fig. 4. EDX line-scan for 90 vol % cBN sample sintered under p = 8 GPa and T = 2400 °C: N$K\alpha_{1_2}$ (*1*), Si$K\alpha_1$ (*2*), Ti$K\alpha_1$ (*3*), B$K\alpha_{1_2}$ (*4*), C$K\alpha_{1_2}$ (*5*).

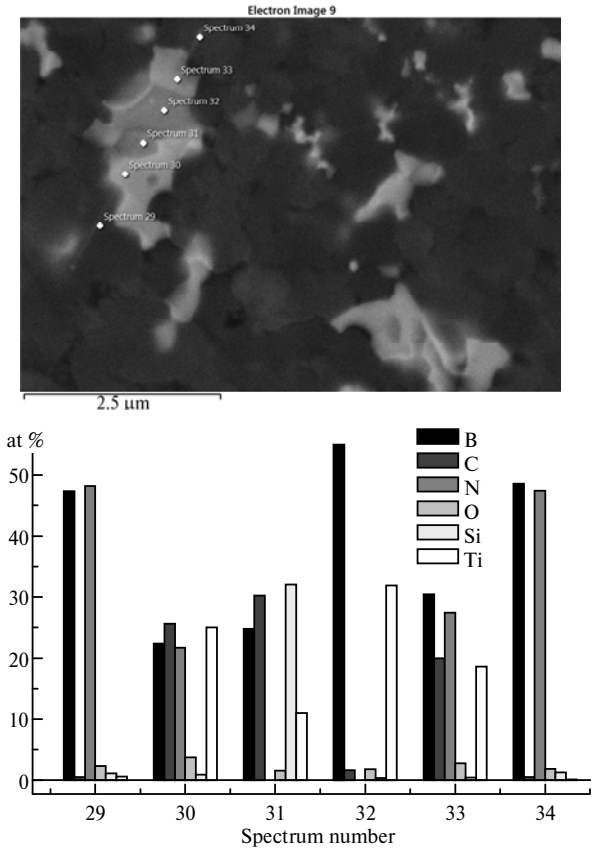

Fig. 5. EDX point analysis for the region shown in Fig. 4.

In our case, the list of the initial components is slightly wider than the one for reaction (2) due to the presence of minor amounts of graphite in the original mixtures.

Only very weak reflections of the SiC phase were found in the XRD (see Fig. 2). The TiB_2 and SiC presence was confirmed via the EDX and XRD (Fig. 5). The presence of amorphous silicon, however, was not confirmed in this study. The EDX mapping presented in Fig. 6 shows that even at high sintering temperature $TiSi_2$ phase remains stable but not seen using the XRD, as it most likely has amorphous nature.

Figure 6 also confirms a high oxygen content in the material microstructure. The XRD does not show the presence of oxide phases and this indicates a dissolution of surface oxygen into the binder phases [6].

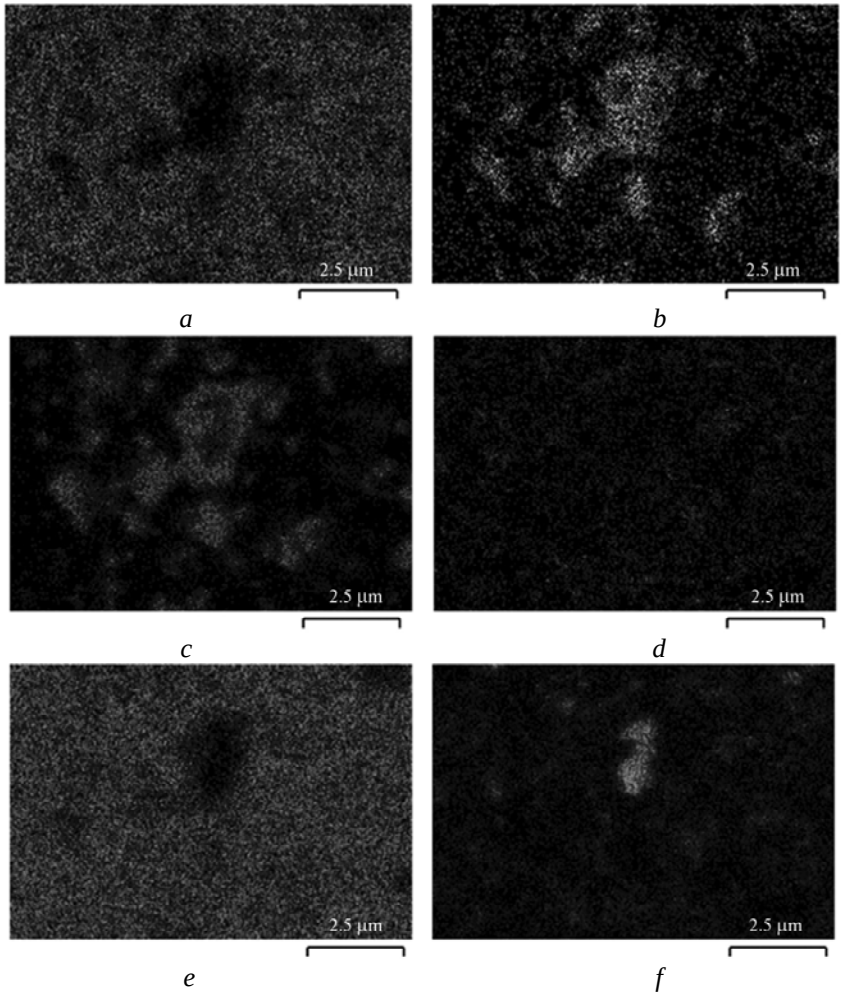

Fig. 6. EDX mapping of the sample with 80 vol % of cBN in the initial mixture (p = 8 GPa and T = 2200 °C): B$K\alpha_{1_2}$ (*a*), C$K\alpha_{1_2}$ (*b*), Ti$K\alpha_1$ (*c*), O$K\alpha_1$ (*d*), N$K\alpha_{1_1}$ (*e*), Si$K\alpha_1$ (*f*).

Microstructure

The formation of a matrix for sintered samples is determined by the compositions of the initial mixtures. 90 vol % of cBN samples received a predominantly cBN matrix with separate inclusions of products of Ti_3SiC_2 decomposition and reaction. In the case of 60 vol % cBN sample the matrix is fully realized through the Ti_3SiC_2 decomposition and reaction products described in the previous section. An intermediate situation was observed for 80 vol % cBN

samples. However, the main influence on the obtained microstructure was observed from the sintering temperature.

The general tendency for the influence of sintering temperature follows the next pattern. In the temperature range of 1400–1600 °C the decomposition of Ti_3SiC_2 leads to the formation of products, which react with cBN; that is visible as rounding of cBN grains. At 1800 °C the initial sintering between cBN grains was observed, while at 2000 °C the formation of nano- and micro-pores appears on the grain boundaries. At 2200–2400 °C the pores grow in size and have a tendency to move to triple junctions (Fig. 7). Neither total recrystallization, nor grain growth or grain coarsening was detected for cBN phase even at 2400 °C.

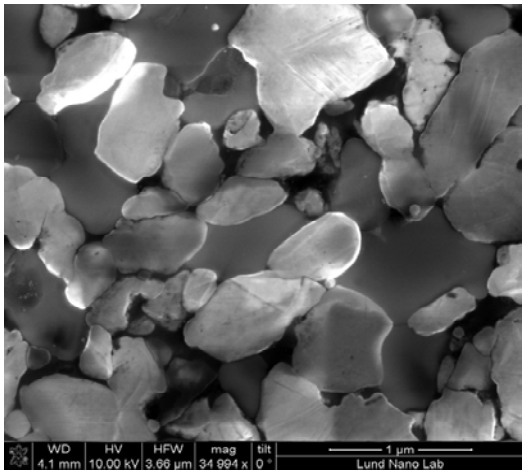

Fig. 7. SEM image of the microstructure for the sample with 80 vol % cBN sintered at T = 2400 °C.

The sintering temperature has more prominent effect on the Ti_3SiC_2 binder component than on the cBN phase. Morphology of this binder component changes in the following way: the MAX-phase decomposition in the region of T = 1400–1600 °C results in the formation of submicron grains (Fig. 8) of phases described in the earlier sections. At T = 1600–1800 °C the recrystallization and grain growth processes begin.

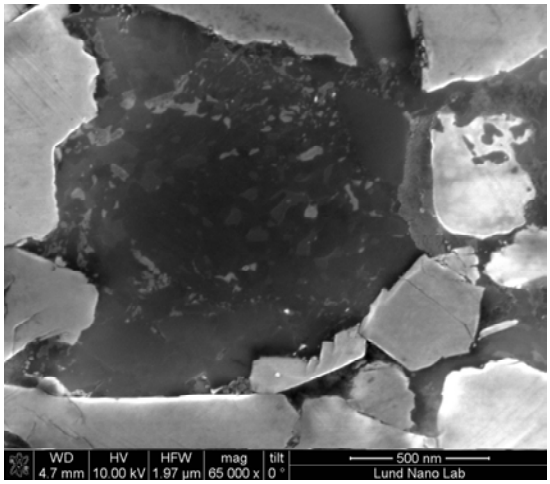

Fig. 8. SEM image of the microstructure for the 60 vol % cBN sample sintered at T = 1400 °C.

At temperatures above 1800 °C the microstructural transformation of the decomposition and reaction products of Ti_3SiC_2 MAX-phase looks to be complete where a clear separation of TiC, TiB_2, SiC, Ti(C,N) phases is observed (Fig. 9). This is accompanied by the formation and growth of pores on triple junctions. It should be mentioned that some of the spheroidal grains, as shown in Fig. 8, were present in the binder even at 2400 °C. Decomposition and reaction products of Ti_3SiC_2 demonstrate the start of the recrystallization at temperatures by approx. 200–300 °C earlier.

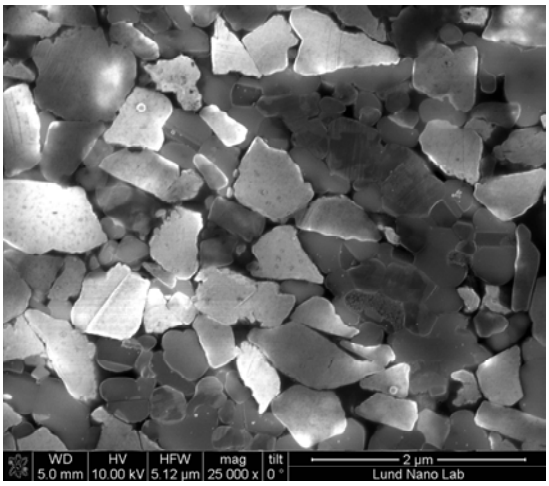

Fig. 9. SEM image of the microstructure for the 60 vol % cBN sample sintered at T = 2000 °C.

Being sintered above 1800 °C, only samples with lowest cBN content show density decreasing (Fig. 10). This can be related to the formation of multiple pores in the microstructure, and also to volume changes due to the formation of new phases as a result of a complete decomposition the (see Fig. 9).

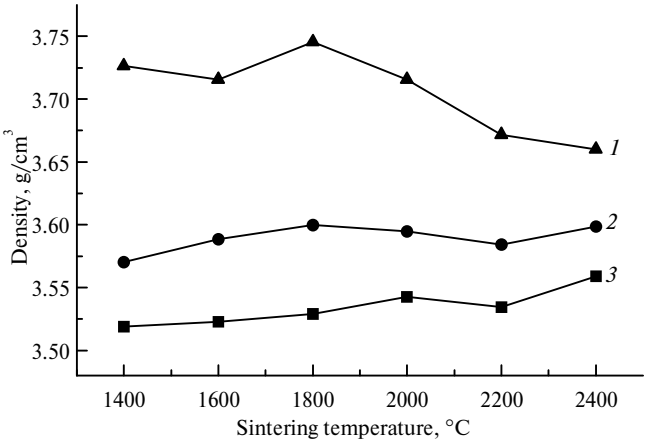

Fig. 10. Average density variations for different sintering temperatures and cBN content: 60 (*1*), 80 (*2*), 90 (*3*) vol % cBN.

The microhardness and fracture-toughness changes closely follow (Figs. 11 and 12) the behavior of the sample density.

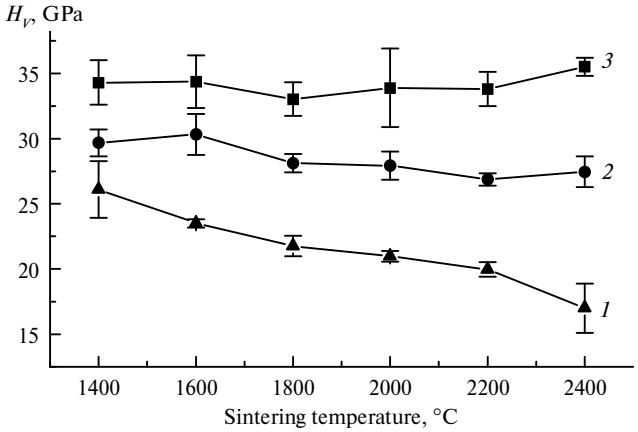

Fig. 11. Microhardness variations for different sintering temperatures and cBN contents: 60 (*1*), 80 (*2*), 90 (*3*) vol % cBN.

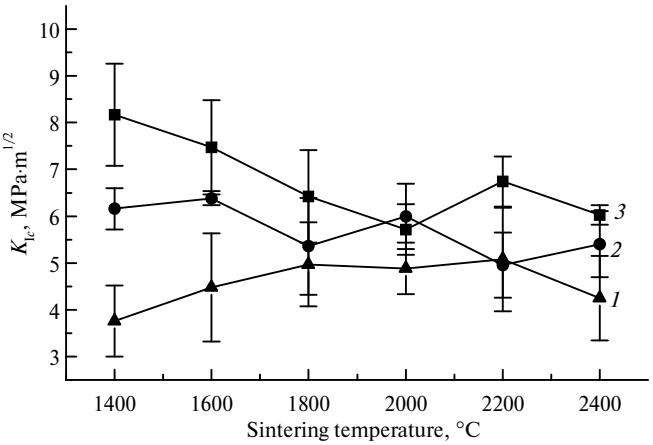

Fig. 12. Fracture toughness variations for different sintering temperatures and cBN contents: 60 (*1*), 80 (*2*), 90 (*3*) vol % cBN.

It shows that for high-cBN samples the hardness does not change significantly with the sintering temperature but for low-cBN samples it is decreasing. This is most likely to be related to the formation of porosity in the sample microstructure. The indentation fracture toughness for the low-cBN sample is the lowest among the obtained cutting tool materials.

Cutting performance

A series of samples with the highest mechanical properties were selected for the estimation of their application performance in machining. The results of the cutting tests, alongside with respective mechanical properties, are listed in Table 2.

The results show that the materials with the lowest cBN content (60 vol % cBN) and with the highest cBN content (90 vol % cBN) exhibit the best performance in terms of wear resistance to the formation of a crater on the rake face (*KT*) and flank wear (*VB*). More descriptive information on the correlation between mechanical properties and machining performance for samples with 60, 80, and 90 vol % cBN sintered at 2000 °C is shown in Figs. 13 and 14.

Table 2. Results of the cutting test for samples having the best mechanical properties

cBN content, vol %	T, °C	H_V, GPa	K_{Ic}, MPa·m$^{1/2}$	KT, μm	VB, μm
80	1600	30.3	6.4	55	157
90	2000	33.8	5.7	58	190
80	2000	30.0	6.0	83	269
60	2000	21.0	4.9	70	183
90	2400	35.5	6.0	44	167
90	2200	33.8	6.7	–	–

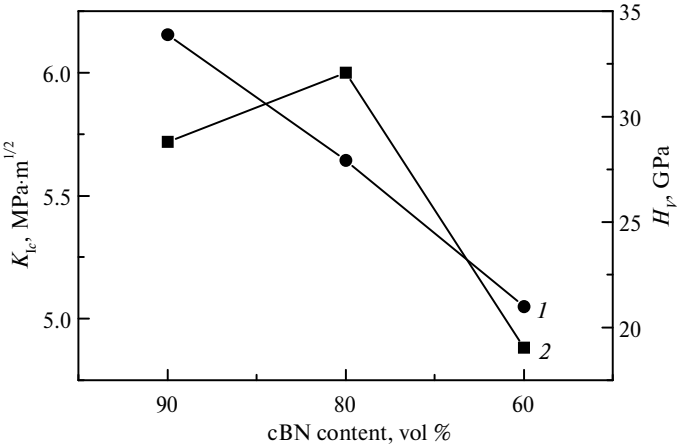

Fig. 13. Microhardness (*1*) and fracture toughness (*2*) for samples sintered at 2000 °C.

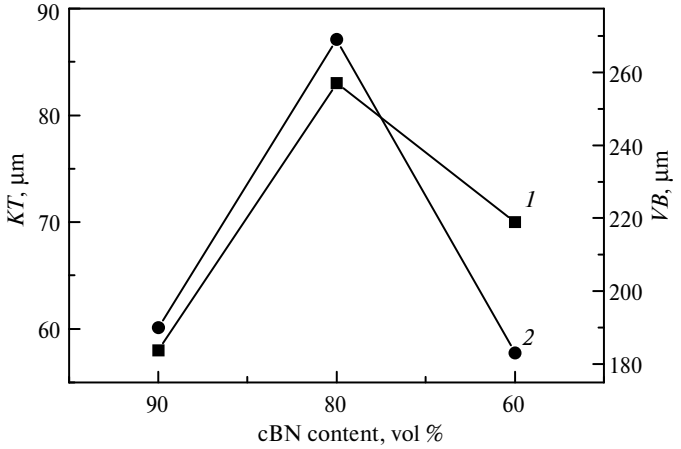

Fig. 14. Crater depth *KT* (*1*) and flank wear *VB* (*2*) for samples sintered at 2000 °C.

These diagrams show that the fracture toughness, which more closely reflects microstructural transformations and the present defects, is more indicative of tool performance in hard turning.

CONCLUSIONS

This study addresses the HPHT sintering of superhard composite materials in the system of cubic boron nitride with Ti_3SiC_2 MAX-phase binder. Three systems

of varying cBN content sintered in the temperature range of 1400–2400 °C are studied.

The mechanisms of the decomposition of Ti_3SiC_2 at the temperature of sintering govern the formation of binder matrices for the studied composites. The decomposition products were found to enter into the reactions with the superhard cBN phase. The following products that create the binder matrix were found via XRD and EDX analyses: TiC, Ti(C,N), SiC, TiB_2. Additionally, in the lower temperature range of 1400–1600 °C the products of incomplete decomposition, such as $TiSi_2$ and Si were also observed. The formation of pores in triple junctions was observed for all samples, yet the most intensive formation was found for low cBN (60 vol %) content samples. This was associated with volumetric change observed when intermediate decomposition products were transformed into Ti(C,N), SiC, and TiB_2–based matrix.

The best combination of mechanical properties for cBN–Ti_3SiC_2–TiC fine-grained tool materials was obtained for the sintering temperature range of T = 1800–2200 °C.

This work was co-funded by the European Union's Horizon 2020 Research and Innovation Program under Flintstone2020 project (grant agreement No 689279). It is also a part of the strategic research program of the Sustainable Production Initiative SPI, involving cooperation between the Lund University and the Chalmers University of Technology. The author (TK) wishes to acknowledge the support provided by the Swedish Institute scholarship.

Надтверді матеріали системи cBN–(Ti_3SiC_2–TiC) при високому тиску і високій температурі. Спікання проводили при тиску 8 ГПа в температурному діапазоні 1400–2400 °C. Вихідні суміші трьох композицій були обрані з вмістом cBN 90, 80 і 60 % (за об'ємом). Суміші були приготовані шляхом змішування cBN (1–3 мм) и Ti_3SiC_2–TiC (< 2 мм). Було встановлено, що після спікання в результаті хімічних реакцій склад отриманих зразків відрізняється від складу вихідних сумішей. Проводили спостереження мікроструктури, оцінку фазового складу і механічних властивостей отриманих інструментальних матеріалів. Результати вказують на те, що різний зміст cBN і застосовані умови спікання чинять прямий вплив на структуру, властивості і кінетику реакцій.

***Ключові слова**: pcBN, Ti_3SiC_2 MAX-фаза, HPHT.*

Сверхтвердые инструментальные материалы системы cBN–(Ti_3SiC_2–TiC) были спечены при высоком давлении и высокой температуре. Спекание проводили при давлении 8 ГПа в температурном диапазоне от 1400 до 2400 °C. Исходные смеси трех композиций были выбраны с содержанием cBN 90, 80 и 60 % (по объему). Смеси были приготовлены смешиванием порошков cBN (1–3 мм) и Ti_3SiC_2–TiC (< 2 мм). Было установлено, что после спекания в результате химических реакций состав полученных образцов во всех случаях отличается от состава исходных смесей. Проводили наблюдения микроструктуры, оценка фазового состава и механических свойств полученных инструментальных материалов. Результаты указывают на то, что разное содержание cBN и применяемые условия спекания оказывают прямое влияние на структуру, свойства и кинетику реакций.

***Ключевые слова:** pcBN, Ti_3SiC_2 MAX-фаза, HPHT.*

1. *Haplin T., Byrne G., Barry J., Ahearne E.* The performance of polycrystalline cubic boron nitride tools in continuous, semi-interrupted, and interrupted hard machining // J. Eng. Manuf. – 2009. – **223**. – P. 947–953.
2. *Bushlya V. M., Gutnichenko O. A., Zhou J. M.* et al. Tool wear and tool life of PCBN, binderless cBN and wBN–cBN tools in continuous finish hard turning of cold work tool steel // J. Superhard Mater. – 2014. – **36**, N 1. – P. 49–60.

3. *Bushlya V. Gutnichenko O., Zhou J. et al.* Effects of cutting speed when turning age hardened Inconel 718 with PCBN tools of binderless and low-CBN grades // Mach. Sci. Technol. – 2013. – **17**, N 4. – P. 497–523.
4. *ISO 1832:2012.* Indexable inserts for cutting tools – Designation.
5. *Barsoum M. W., Brodkin D., El-Raghy T.* Layered machinable ceramics for high temperature applications // Scripta Materialia. – 1997. – **36**, N 5. – P. 535–541.
6. *Angseryd J., Elfwing M., Olsson E., Andrén H.-O.* Detailed microstructure of a cBN based cutting tool material // Int. J. Refract. Met. Hard Mater. – 2009. – **27**, N 2. – P. 249–255.
7. *Zhu Y., Jia J., Zhou A. et al.* Sintering of Ti_3SiC_2 ceramics by hot press from commercial powders // Proc. 5th Int. Congress on Ceramics (ICC5), Beijing, China, 17–21 August, 2014, publ. in Key Eng. Mater. – 2014. – **655**. – P. 68–71.
8. *Li Z., Zhou A., Li L. et al.* Synthesis and characterization of novel Ti_3SiC_2–cBN composites // Diamond Relat. Mater. – 2014. – **43**. – P. 29–33.
9. *Benko E., Klimczyk P., Mackiewicz S. et al.* cBN–Ti_3SiC_2 composites // Diamond Relat. Mater. – 2004. – **13**, N 3. – P. 521–525.
10. *Xue Y., Qin J., Zhang X. et al.* In situ high pressure synthesis of cBN-based composites // Funct. Mater. Lett. – 2014. – **7**, N 4, art. 1450040.
11. *Mu Y., Guo J., Liang B., Wang Q.* Rapid fabrication of the Ti_3SiC_2 bonded diamond composite by spark plasma sintering // Int. J. Refract. Met. Hard Mater. – 2011. – **13**. – P. 397–400.
12. *Mu Y.-C., Han J.-X., Liu J.-L. et al.* Microstructure of Ti_3SiC_2/diamond composite materials prepared by hot-pressing // Fenmo Yejin Cailiao Kexue yu Gongcheng/Mater. Sci. Eng. Powder Metal. – 2015. – **1**. – P. 139–143.
13. *Rampai T., Lang C. I., Sigalas I.* Investigation of MAX phase/c-BN composites // Ceram. Int. – 2013. – **39**, N 5. – P. 4739–4748.
14. *Zhou A., Li Z., Li L. et al.* Preparation and microstructure of Ti_3SiC_2 bonded cubic boron nitride superhard composites // Kuei Suan Jen Hsueh Pao/J. Chinese Ceram. Soc. – 2014. – **42**, N 2. – P. 220–224.
15. *Qin J., He D.* Phase stability of Ti_3SiC_2 at high pressure and high temperature // Ceram. Int. – 2013. – **39**, N 8. – P. 9361–9367.
16. *Advances* in Ceramic Matrix Composites: Woodhead Publishing Series in Composites Science and Enginee / Ed. I. M. Low. – Elsevier Science & Technology, 2014. – 734 p.
17. *Khvostantsev L. G., Slesarev V. N.* High pressure apparatuses of a high volume for physical investigations // Physics-Uspekhi. – 2008. – **178**, N 10. – P. 1099–1104.
18. *Taniguchi T., Akaishi M., Yamaoka S.* Mechanical properties of polycrystalline line translucent cubic boron nitride as characterized by the Vickers indentation method // J. Am. Ceram. Soc. – 1996. – **79**, N 2. – P. 547–549.

Received 06.03.17